Full paper / Mémoire

Localized electrochemical techniques: Theory and practical examples in corrosion studies

Stefano Rossi*, Michele Fedel, Flavio Deflorian, Maria del Carmen Vadillo

Department of Materials Engineering and Industrial Technologies, University of Trento, Via Mesiano 77, 38050 Trento, Italy

Abstract

   This paper aims at giving an idea of the contributions to the study of corrosion phenomena ensured by the practice of localized electrochemical techniques. For many corrosion phenomena high resolution is required. This is due to the fact that a huge amount of relevant information about electrochemical processes can be examined at a microscale.

   The present work is focused both on theoretical and practical aspects of these modern localized electrochemical techniques. In particular Scanning Kelvin Probe (SKP) and Scanning Vibrating Electrode Technique (SVET) will be discussed in detail. Concerning theoretical aspects, this paper summarizes in some fundamental equations the main operating principles behind the two different techniques. The basics of the two equipments are explained in simple terms with the aid of some pictures. Experimental data are also reported, in order to better understand the working principles of these devices and their potential. The novelty of the data obtained with these tools will be highlighted by the discussion of the theoretical principles and the explanation of several examples. *To cite this article: S. Rossi et al., C. R. Chimie 11 (2008).*

1. Introduction

   Nowadays corrosion scientists and engineers use a huge number of electrochemical techniques that enable them to obtain much information about reactions at the solid/liquid and the solid/gas interface. For this purpose simple DC current experiments, just a simple potential vs time measurement gives useful information on the corrosion processes. If more complete data are required, it is possible to perform potentiodynamic experiments in order to understand properly the electrochemical behaviour of the studied systems.

   These techniques are simple and quite cheap but they do not supply enough information to explain completely the corrosion phenomena, in particular concerning polymer/metal composites [1,2]. Improvements to the corrosion study came out after the introduction of the AC current techniques or rather electrochemical impedance spectroscopy (EIS). This very powerful tool has been largely used for the interpretation of many of corrosion processes, both on bare and coated (organic or inorganic coatings) metals [3].

   All these techniques have been used for years and nowadays they are well known and widespread in every corrosion control laboratory.

   In spite of this, these tools have an important limitation, i.e. the spatial resolution. Using these techniques it

   * Corresponding author.
      E-mail address: rossi.stefano@ing.unitn.it (S. Rossi).

is possible to achieve only average data about the behaviour of an electrochemically active surface. It is very difficult to apply these techniques and the associated analysis models to small surface areas. For example, it is not possible to differentiate small local anodes and cathodes on a metal surface or to detect precisely filiform corrosion phenomena. This means that it is necessary to apply different strategies in order to investigate these kinds of processes on the microscale. In the last two decades a lot of efforts have been made in order to realize new equipments for the analysis of corrosion phenomena with high spatial resolution. Scanning Kelvin Probe (SKP), Scanning Kelvin Probe Force Microscope (SKPFM), Scanning Vibrating Electrode Technique (SVET) and Localized Electrochemical Impedance Spectroscopy (LEIS) are the main results of all these attempts. LEIS is the evolution of the traditional Electrochemical Impedance Spectroscopy. With this technique it is possible to investigate the interfacial impedance properties of bare or coated metals. The influence of heterogeneities on the surface of bare metal samples can be investigated as well as the presence of blisters on coated metal samples [4,5].

SKP, SKPFM and SVET equipment enable the measurement of local potential and current difference on the microscale [6]. SKP is a non-contact and non-destructive device that allows us to measure and map the work function difference between a sample and a reference probe using the vibration condenser method. SKPFM is a very similar device. The physical working principle is the same as SKP, but the resolution is higher because the probe is much smaller than the probe used in the classical SKP [7]. Similar to the SKP, the SKPFM allows mapping of topography and Volta potential difference distribution on the investigated sample's surface [8].

SVET is an electrolyte immersed device that enables us to spatially characterize corrosion activity measuring the potential gradients in the electrolyte (using a fine tipped vibrating microelectrode) due to the presence of anodic and cathodic areas on a metal surface.

Among these techniques, the SKP and the SVET seem to be much more appreciated by the scientific community than LEIS and SKPFM. In fact, despite LEIS being a very promising technique, several questions on the correct interpretation of the experimental data still influence the diffusion of this device. Concerning SKPFM, it has been demonstrated [7] that this technique is subject to much more artefacts than the classical SKP. At the moment, the information obtained using SVET and SKP seems to be the object of major interest. In fact, using these equipments it is

possible to investigate metal samples at the micrometer scale level and to obtain very useful information on the physics and/or chemical reactions occurring on the surface [9]. With the aid of these devices it is possible to analyse a huge number of electrochemical processes and to check a lot of different materials (they are used on metals, semiconductors and polymers).

Several studies have been performed using the SKP [10–12] and SVET [13–15] technique. For example, SKP has been used for studying corrosion problems under thin and ultra-thin electrolyte layers and at the buried interface organic coating/metal [7], for the detection of residual stresses and inclusions on metal surfaces [16] and for the study of thin hybrid conversion films [17].

On the other hand SVET has been used for the corrosion control and analysis of a Zn–Al alloy galvanised coatings [18], for the study of electroactive conducting polymers [19] and for the evaluation of corrosion resistance of siloxane coatings [20].

Because of the great potential and the increasing interest for high resolution techniques in corrosion studies, the theory and practice of SKP and SVET will be discussed in the next chapters. All measurements were recorded using a SVP/SKP100E (by Perkin Elmer Instruments) system at normal conditions in the Industrial Corrosion Control Laboratory at the University of Trento (Trento, Italy).

2. Scanning Kelvin Probe

2.1. The technique

The Scanning Kelvin Probe technique measures micro-galvanic activity existing close to the surface of an electrochemically active specimen in the presence of a film or a drop of electrolyte or in humid air. It is a non-contact, non-destructive device for the determination of the work function of conducting and semiconducting materials. The scanning tip is a cylindrical Platinum wire ($\varnothing = 500\ \mu m$). It is important to note that SKP is a unique device able to investigate corrosion processes without the employment of a conducting liquid media. As anticipated before, it works in air as well as in the presence of drops of electrolyte.

After the development of the principles of direct correlation between the measured work function and the surface condition [21], it became a tool of wide application for both surface science and industrial uses. Regarding corrosion science and electrochemistry, the technique permits the investigation of different fields such as localized corrosion phenomena, surface

coating degradation, effect of microstructure and finish on corrosion initiation, the performance of corrosion inhibitors, the performance of batteries and, in general, the behaviour of materials in aggressive environments.

2.2. Theory behind the SKP technique

The orientation of the Kelvin Probe tip with respect to the sample surface approximates a parallel plate capacitor (see Fig. 2) where the capacitance C is defined by Eq. (1):

$$C = \frac{\varepsilon \varepsilon_0 A}{d} \tag{1}$$

where ε_0 is the dielectric constant, ε is the dielectric permittivity of the gas in between the plates, A is the area of the SKP tip and d is the distance between the plates. The presence of a little quantity of opposite charge on the surface of the tip and on the surface of the sample is a direct consequence of the electrical connection between the two. Evidence of this will be provided shortly.

The position of the KP tip changes with time and hence:

$$d(t) = d_0 + d_1 \sin(\omega t) \tag{2}$$

where d_0 is the average distance between the SKP tip and the sample surface, d_1 is the amplitude of vibration and t is time in seconds. The frequency at which the probe vibrates is ω expressed in radians. Current flows through the capacitor via an external circuit when there is a non-zero potential difference ΔE between the KP and the sample. The current i, assuming a homogenous electric field between the plates, can be expressed as:

$$i = \frac{dQ}{dt} = \Delta E \frac{dC}{dt} \tag{3}$$

Substituting Eqs. (1) and (2) in Eq. (3), the current signal $i(t)$ can be expressed as:

$$i(t) = \varepsilon \varepsilon_0 A \Delta E \frac{d_1 \omega \cos(\omega t)}{[d_0 + d_1 \sin(\omega t)]^2} \tag{4}$$

A non-zero potential difference arises in almost all circumstances, even when identical materials are used for the KP and the sample. Non-equal contributions from the chemical potential of electrons and the surface potential associated with each material give rise to a Volta potential difference.

In this case, the sum of the chemical potential and the surface potential (the work function) for the KP

is much larger than for the sample. Under such circumstances, when the two are connected in an electric circuit, electrons flow from the material of lower work function to that of higher work function (high to low energy) until their respective Fermi energies equalize. The voltage required to reduce the electric field is proportional and of opposite sign to the Volta potential difference $\Delta_S^{KP}\psi$ [21]. By definition then:

$$\Delta E = E_S + \Delta_S^{KP}\psi \tag{5}$$

where E_S is the voltage applied to the sample.

Fig. 1(a–c) illustrates three electron energy diagrams depicting two metals characterized by work function and Fermi level of (ϕ_1, E_1) and (ϕ_2, E_2), respectively. The schemes of Fig. 1 are useful to understand what happens connecting a conductive sample to the Platinum Kelvin Probe.

The diagram on the left (Fig. 1a) shows the metals with no electrical contact. The different Fermi levels are highlighted. When an electrical contact is realized (Fig. 1b) the flow of charge allows the Fermi levels to equalize and gives rise to a surface charge and potential difference V_c, which relates to the difference in work function:

$$-eV_C = \phi_1 - \phi_2 \tag{6}$$

where 'e' is the electron charge. Applying an external backing potential, V_B, (Fig. 1c, on the right) it is possible to nullify the surface charge at the unique point, where $V_B = -V_C$. The SKP system performs this measurement using a vibrating capacitance probe. The backing potential, V_B, is then varied automatically to ensure that the null point is always maintained and thus the potential at which current nullifying occurs equates to the work function difference between the probe and the sample.

In the field of corrosion science, measurements of work function can be taken one step further to allow the corrosion potential (E_{corr}) at a specific point to be determined. Stratmann [22,23] demonstrated the following relationship:

$$E_{CORR} = Cost + \left(\frac{\phi_1 - \phi_2}{e}\right) \tag{7}$$

where $\phi_1 - \phi_2$ is the measured work function difference between the probe and the sample and Cost is a constant. It is possible to calibrate the Scanning Kelvin Probe using a conventional reference electrode of known equilibrium potential in order to find the constant term in
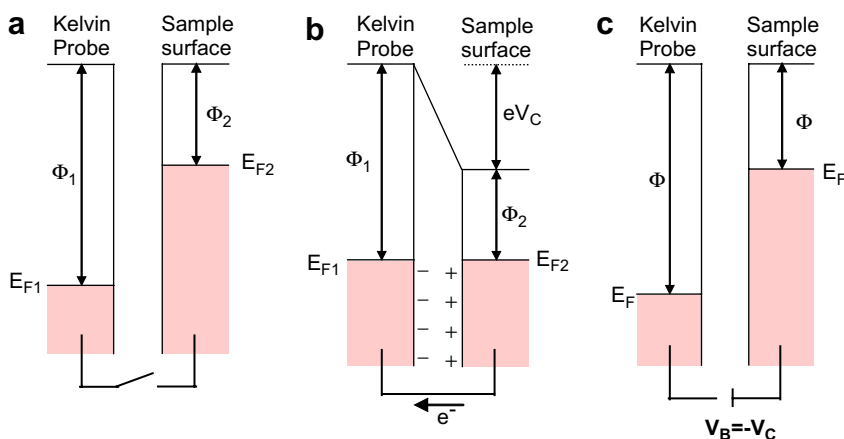
Fig. 1. (a−c) Energy level diagrams illustrating the basics of the SKP.

the above equation [24]. Usually the Volta Potential is measured with respect to the Cu^{2+}/Cu couple, in order to easily calibrate it vs the standard reference electrode (Cu^{2+}/Cu +0.34 vs SHE) [8,25].

Without going into details, it is also possible to perform topographical measurements using the difference capacitance between the probe and the sample to determine the height of the probe above the surface being scanned [26]. It is achievable by means of a suitable "height calibration".

2.3. Practical example of SKP measurements

In the following, practical examples of some applications of this technique will be presented. In order to put the right emphasis on the non-destructive feature of this device, it is important to note that all reported measurements have been performed in air without the presence of an electrolyte.

2.3.1. Organic coated steel food-cans
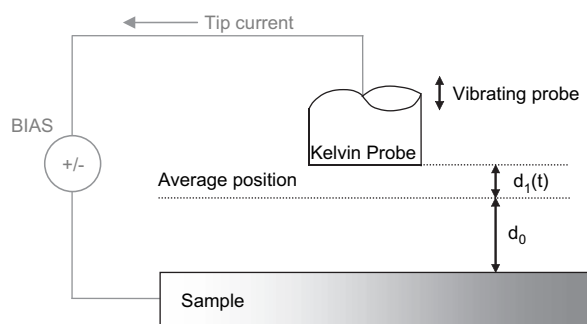The first example deals with the investigation of localized defects in food industry organic coatings. In

particular, two different food-cans protective coatings such as TiO_2 enriched melaminic coating and TiO_2 and carbon black enriched phenolic coating have been analysed. For both the two coatings the substrate consists of tin plated mild steel. Measurements have been performed before and after the immersion of the sample in a 0.35 wt% NaCl solution (pH modified to 4 adding HCl) for 120 h. This solution simulates the corrosion attack of vegetables and fruit acids, in order to better highlight the real damage that can occur.

For comparison an SKP measurement has been also performed on a bare tin plated surface. Fig. 3 shows the results of the measurement. In this case the scanned area is 15.0×19.4 mm. The surface looks quite homogenous, even if some little defects (or discontinuity) are observable. In fact the value of the work function difference mainly attests around the mean value.

For the investigation on the organic coated surface the set scan area is 25.5×19.0 mm. Fig. 4 shows the

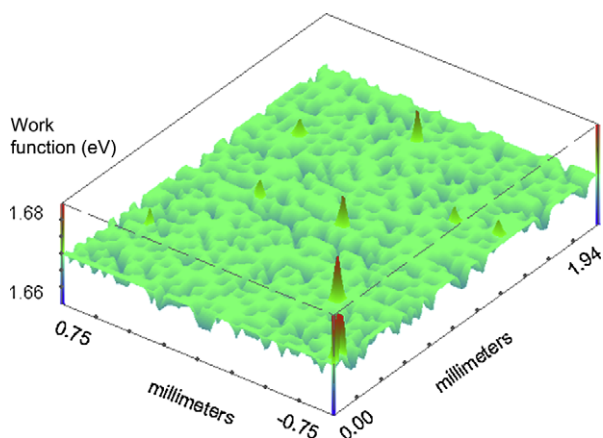Fig. 2. Schematic representation of the SKP vibrating system.

Fig. 3. SKP in topography mode for a tinplate surface: three-dimensional representation.
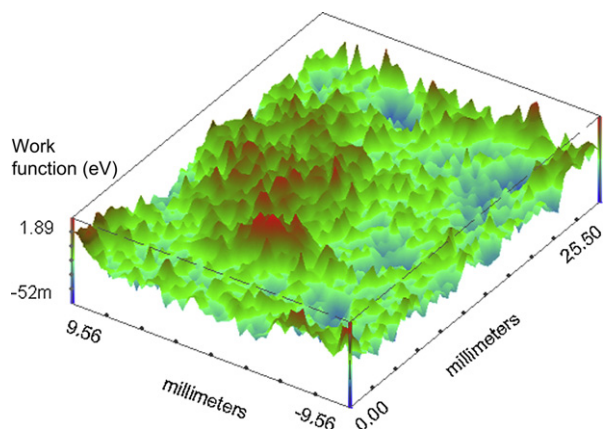
Fig. 4. Working Function difference map of the base of the melaminic coating covered container before continuous immersion in the 0.35 wt% NaCl solution at pH 4.

Fig. 6. Working Function difference map of the base of melaminic organic coated container after 120 h of continuous immersion in the 0.35 wt% NaCl solution at pH 4.

melamine coated container base before the continuous immersion. It is possible to observe some defects on the surface represented by high and localized work function variation, compared with the average value all over the surface (1 deV, with a standard deviation of 0.21). Fig. 5 presents the SKP map of the phenolic polymer coated container base before immersion in the electrolytic solution. Comparing this mapping with the previous (Fig. 4) it is clear that, except for the marginal zones, the total area is more homogeneous than the corresponding melaminic coated food-can. The average value for the phenolic before continuous immersion is 0.4 deV with a standard deviation of 0.3. Fig. 6 shows the representative behaviour of the melaminic coated food-can after continuous immersion for 120 h. The average work function difference is 2 deV with a standard deviation of 0.62. It is possible to

observe that the coating surface is damaged by the chloride ions generating some defects. Fig. 7 shows the phenolic coated surface after the immersion in the electrolytic solution. Its work function average value is 1.1 deV and the standard deviation is 0.98.

With these results it is possible to observe more important changes on the melaminic coating compared to the phenolic one. Considering the impedance data reported in Fig. 8, it is evident that the melaminic coating has better barrier properties than the phenolic coating. This fact confirms the SKP analysis, because the melaminic coating lacks homogeneity and is characterized by a high number of defects (highlighted by scattering of the work function difference). In addition note that both the analysis confirm that after the immersion time the two coatings look very similar and there are no remarkable differences between them. This example
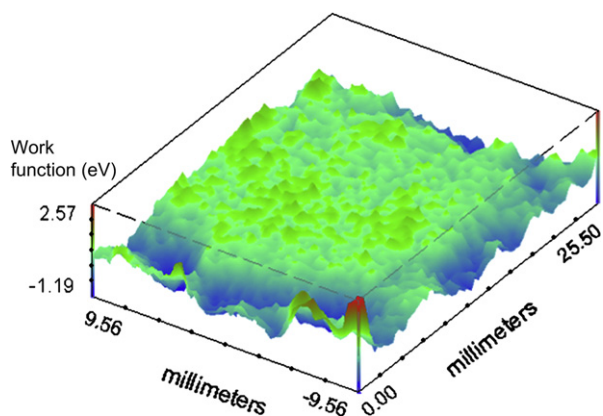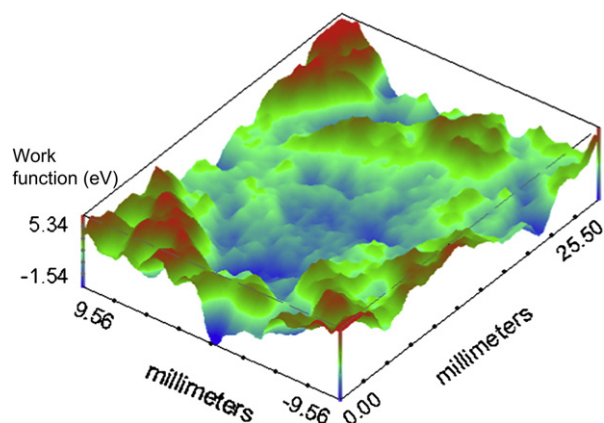

Fig. 5. Working Function difference map of the phenolic organic coated container before continuous immersion in the 0.35 wt% NaCl solution at pH 4.
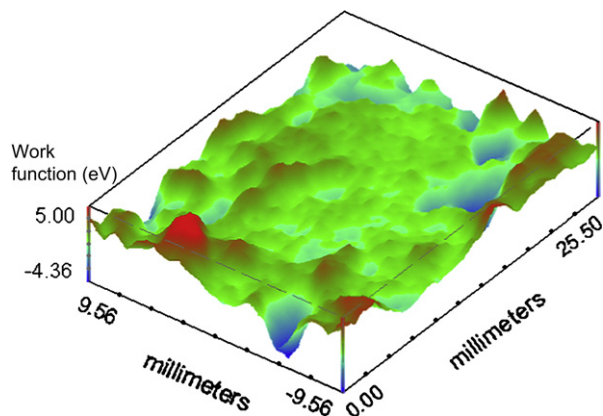

Fig. 7. Working Function difference map of the phenolic organic coated container after 120 h of continuous immersion in the 0.35 wt% NaCl solution at pH 4.
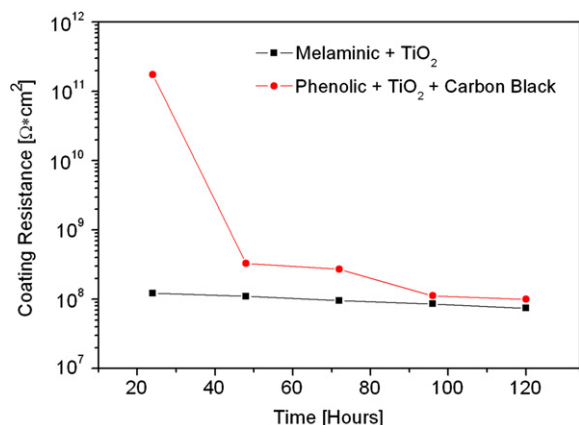
Fig. 8. Coating resistance after 120 h of immersion in the electrolyte.

proves that SKP is a very useful tool for the investigation of coating defects and, with respect to EIS, it provides a finer analysis of the surface conditions of the organic coatings.

2.3.2. Hybrid silane conversion film

Applying a simple statistical analysis to the SKP experimental data it is possible to obtain more refined data about the studied system. In this example several SKP measurements were performed on silane treated copper panels. Silanes are hybrid molecules (widely used as adhesion promoters between inorganic and organic materials) able to form a thin film on metals surfaces [27]. It is possible to obtain the conversion coating by dipping copper panels into a water based solution containing silanes molecules and curing the self-assembled films in an oven for a certain time and temperature combination.

Table 1 shows the different kinds of deposition. Ox is a modified commercial mixture of silane molecules (the main fraction consist in γGlycidoxypropyltriethoxysilane, γGPS) while γGPS is the neat single silane molecule.

Fig. 9(a) and (b) depicts SKP results on bare copper (a) and on sample Ox_{10}^5 (b) [28]. Since work function
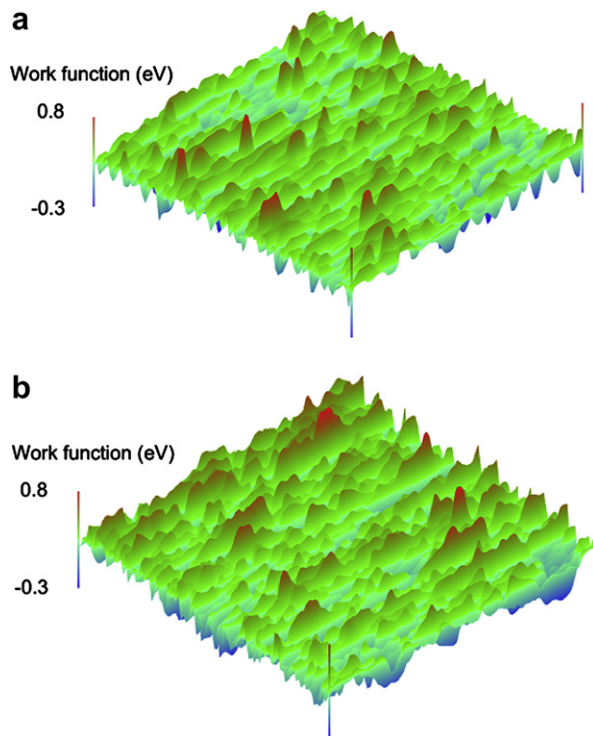

Fig. 9. SKP work function mapping on copper surface (a) and on sample Ox_{10}^5 (b); scan area 15 mm × 15 mm.

mapping gives only a rough idea of the behaviour of different samples, a statistical analysis is necessary, in order to highlight properly the main differences among the different samples. Fig. 10 shows the main values of the work function difference and its standard deviation calculated over the surface of each sample. Note that the relative stability of copper oxide leads to very similar and hardly comparable values of the absolute values of the

Table 1
Silane coated samples: features and labels

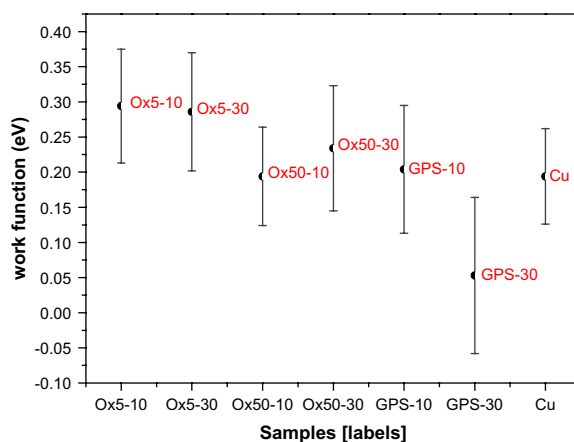| Sample	Silane pre-treatment		Heat treatment (*T* and *t*)
	Type	Concentration (in water)	
Ox_{10}^5	Ox	5%	200 °C, 10 min
Ox_{30}^5			200 °C, 30 min
Ox_{10}^{50}	Ox	50%	200 °C, 10 min
Ox_{30}^{50}			200 °C, 30 min
$γGPS_{10}$	γGPS	5%	200 °C, 10 min
$γGPS_{30}$			200 °C, 30 min

Fig. 10. Average work function values and the corresponding standard deviation.

mean work function difference. For this reason standard deviation was used as an indicator of the surface stability and homogeneousness. Considerable values of this statistical parameter mean a high scattering of work function over the investigated surface. For comparison, Fig. 11 shows the values of the charge transfer resistance for all the investigated samples measured after 1 h of immersion in a 0.3 wt% Na$_2$SO$_4$ solution. This electrochemical parameter has been calculated applying the suitable electrical equivalent circuit model for the elaboration of the impedance data. Considering Figs. 10 and 11 it is easy to observe a very similar hierarchy for the work function and the charge transfer resistance, respectively.

This is to underline the potential of this technique which enables to get precious information about the electrochemical activity of the metal-coating interface. Higher potentials are directly correlated with a more noble behaviour while higher charge transfer resistance means higher corrosion resistance.

Now it is easy to demonstrate that panels treated with neat γGPS show the worst behaviour. Absolute values of the work function for the panels obtained from Ox^5 and Ox^{50} solutions do not look very different and the standard deviation is more or less the same. This simple statistical analysis highlights the fine differences among different depositions. The three-dimensional contact potential map is not sufficient if the aim of the work is an accurate samples characterization.

2.3.3. PVD TiN coated steel

A reactive sputtered TiN coated mirror polished steel surface [29] has been analysed using the Kelvin probe instrument. Fig. 12 shows the correspondent
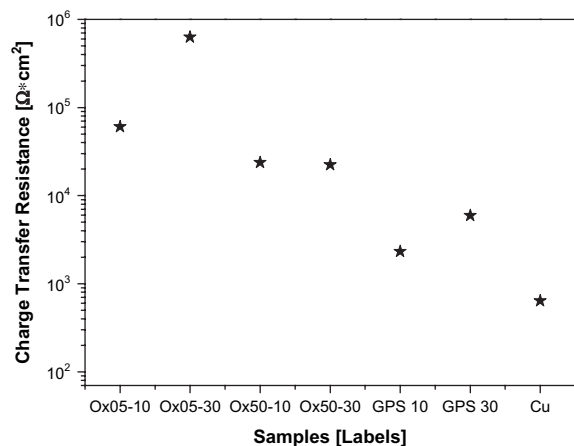
SKP map over a 2.5 × 3.0 mm surface. For comparison, the measurement has been also performed on a portion of the steel sample not covered with the ceramic coating. It is clearly visible (Fig. 12) that there is a different mean work function value for the coated and the bare steel substrate. This is directly connected to the dissimilar electrochemical activity of the different surfaces. This is quite obvious, since we are comparing a ceramic coating with a bare metal. Note that the signal scatters markedly over the whole coated surface. This is a clear clue of the deposit lack of homogeneity. The signal variation (highlighted by the scattering of the work function value) is higher on steel than on the TiN film because of, even if not homogeneous, the ceramic coating which is much more electrochemically stable than the metal. In general, defects occurred during film formation such as cracks or thickness variation could be detected using this technique.

3. Scanning vibrating electrode technique

3.1. The technique

The SVET technique measures the changes in micro-electrochemical activity in proximity of the specimen surface. SVET detects extremely small potential variations which exist over the surface of electrochemically active materials within an electrolyte. For example, this device could be used on stainless steels to determine local conditions within active pits [30]; Bates [31] used this tool for the investigation of pitting corrosion in FV448 gas turbine disc steel and Sekine [32] applied the technique for the evaluation of corrosion protection performance of polymeric resins. In addition, other possible research topics of this technique are pit initiation and development, detecting of

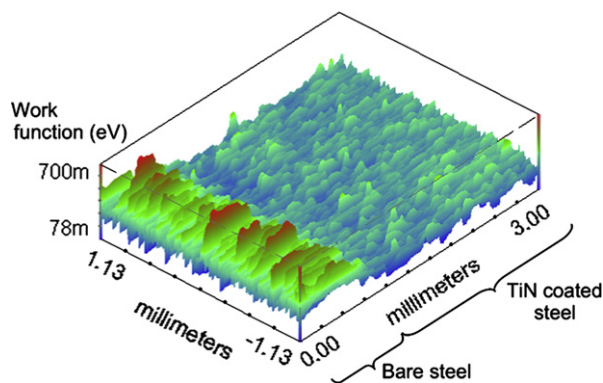Fig. 11. Charge transfer resistance after 1 h of immersion in a 3.5 wt% NaCl solution.

Fig. 12. SKP map over a 3.0 × 2.5 mm area on a PVD TiN coated steel substrate.

electrochemically active pin-hole defects in coatings, effect of microstructure and finish on the electrochemical activity, evaluation of the passivation−repassivation characteristics, corrosion inhibitor performance, micro-corrosion and electrochemical effects, behaviour of materials in aggressive environments.

The technique permits us to obtain potential and current density maps and to quantify the extent of the corrosion processes over the surface of the material under study. It is an in situ working device and allows us to measure localized corrosion events of less than $5 \, \mu A/cm^2$.

The idea to use fine tipped scanning probes to detect changes in micro-galvanic activity close to the specimen surface was proposed by Evans [33]. Later many research groups applied this method to their electrochemistry and corrosion studies [24,34,35].

3.2. Theory behind the SVET technique

Experimentally it has been observed that there exists a flow of metal ions into solution above a localized corrosion phenomenon, and a corresponding flow of electrons within the metal (Fig. 13). This miniature current dipole sets up an associated electric field distribution within the electrolyte. It is the potential variations which SVET detects and quantifies (Fig. 13).

The scanning probe instrument consists of a very thin platinum tip configured as differential inputs to measuring electronics. Tips measure potential variations. The probe scans over a surface of the specimen which is inside the conducting solution (electrolyte). Measurements are made in *x−y* directions, permitting
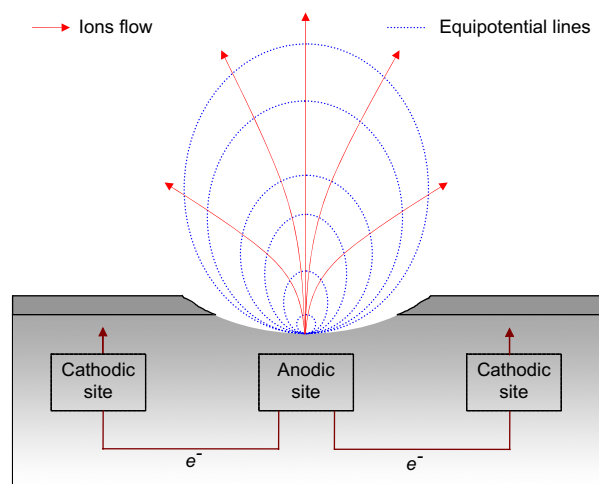
the potential variations of the localized electrochemical activity to be depicted and quantified.

Using a vibrating probe in conjunction with a lock-in amplifier it is possible to eliminate the noise occurring at any frequency other than the frequency of vibration of the probe. This increases the electrical sensitivities and the system stability also improves.

A piezo-ceramic device controls the movements of the probe allowing vibration amplitudes from 1 to 60 μm in the direction perpendicular to the sample surface (Fig. 14).

The explanation of the working principles of this technique is based on the analysis and consideration of Bayet et al. [36]. In their study the microprobe vibrates at an angular frequency of Ω. The distance between the probe and the sample (working electrode) varies with time as follows (see Fig. 15):

$$h(t) = h_0 + d \sin(\Omega t) \tag{8}$$

where d is the amplitude of the probe vibration and h_0 is the average distance between the probe and the sample.

Under galvanostatic control and AC regime, the local current density, $j_{loc}(t)$, just above the electrode surface, can be expressed as:

$$j_{loc}(t) = j_{loc}(t), 0 + \Delta j_{loc} \sin(\omega t) \tag{9}$$

Fig. 13. Current flow and electric field associated with an electrochemically active site on a metal exposed to a conducting solution.
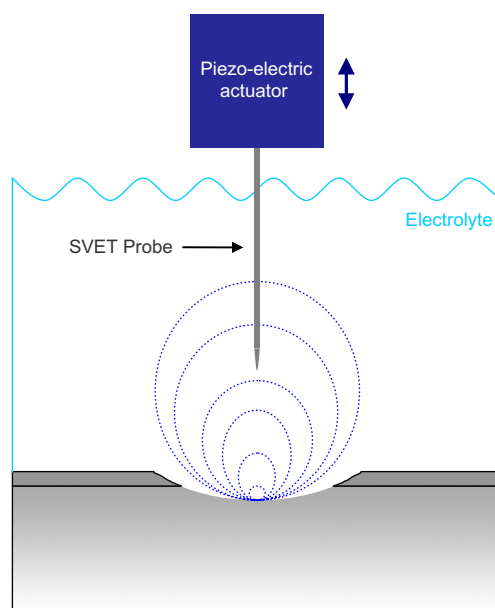

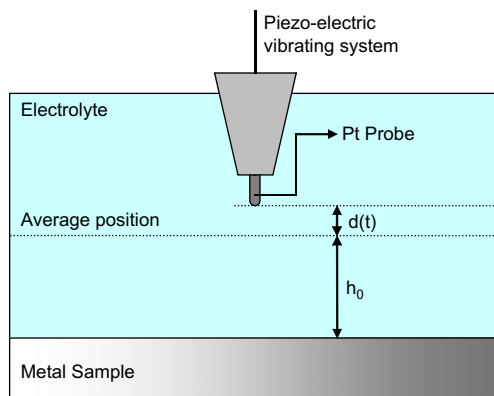
Fig. 14. Schematic representation of the SVET technique.

Fig. 15. Schematic representation of the SVET vibrating system.

where Δ denotes the small AC perturbing component with an angular frequency, ω. The local potential of the interface $E_{loc}(t)$, is given by:

$$E_{loc}(t) = E_{loc},0 + |\Delta E_{loc}(\omega)|\sin(\omega t + \varphi) \qquad (10)$$

where $|\Delta E_{loc}(\omega)|$ is the amplitude of the local potential response at angular frequency ω and φ is the phase shift with respect to j_{loc}. The local complex impedance Z_{loc} can then be defined as:

$$Z_{loc}(\omega) = \frac{|\Delta E_{loc}(\omega)|}{\Delta j_{loc}}e^{j\varphi} \qquad (11)$$

If the electrolyte resistivity, ρ, remains constant even in the vicinity of the sample surface, then the electrolyte resistance relative to the unit surface between the sample surface and the vibrating probe varies with time as follows:

$$R_e(t) = \rho[h_0 + d\sin(\Omega t)] \qquad (12)$$

Therefore the potential between the vibrating probe (VP) and the sample surface (i.e. working electrode, WE) varies with time as follows:

$$\begin{aligned} V_{probe(t)} &= V_{VP} - V_{WE} = E_{loc}(t) + j_{loc}(t)R_e(t) \\ &= [E_{loc},0 + |\Delta E_{loc}(\omega)|\sin(\omega t + \varphi)] \\ &\quad + \rho[h0 + d\sin(\Omega t)][j_{loc},0 + \Delta j_{loc}\sin(\omega t)] \quad (13) \end{aligned}$$

One can readily see that $V_{probe}(t)$ contains both potential $|\Delta E_{loc}(\omega)|$ and current Δj_{loc} information. The difficulty of this approach arises from the fact that V_{probe} is influenced by two different frequencies: the frequency of the probe vibration (Ω) and that used for impedance measurement(ω).

In Eq. (13) the probe signal passes through the electronic circuit as an SVET system. This involves amplification with again G, multiplication by a reference signal $\sin(\Omega t)$ in phase with the probe vibration, and filtering with a low-pass filter with transfer function $F(\omega) = |F(\omega)|\exp(j\Phi F(\omega))$. The signal then passes to the X-input of a frequency response analyser (FRA). Since the correlation calculation performed by the FRA cancels out all signals having a frequency different from ω, the useful component of the signal is from Eq. (13):

$$X(t) = \frac{1}{2}\rho d\Delta j_{loc}G|F(\omega)|\sin(\omega t + \Phi F(\omega)) \qquad (14)$$

On the other hand, the probe signal is sent directly to the Y-input of the FRA. In the same way, Eq. (15) gives the useful component at ω frequency:

$$Y(t) = \rho h_0\Delta j_{loc}\sin(\omega t) + |Z_{loc}|\Delta j_{loc}\sin(\omega t + \varphi) \qquad (15)$$

Hence, the transfer function between the signals $X(t)$ and $Y(t)$ which, respectively, contains the current and potential information can be written as follows:

$$H(\omega) = 2\frac{Z_{loc}(\omega) + \rho h_0}{\rho d G F(\omega)} \qquad (16)$$

The standard calibration operation of the commercial SVET system gives the value of ρd. The $F(\omega)$ and G terms represent the specific filter transfer function and the gain of the commercial SRET circuitry, respectively, and can be readily determined by injection of a known AC signal in the circuit. Thus, the local electrochemical impedance of the interface $Z_{loc}(\omega)$ can be directly obtained from Eq. (16).

3.3. Practical example of SVET measurements

A practical example of SVET measurements will also be reported. An organic coated beverage-can has been studied with the SVET device. Notice that, compared with the Kelvin probe technique, SVET needs an electrolyte directly in contact with the sample surface.

3.3.1. Organic coated steel food-cans

Similar to the SKP measurement, the inner side of the base of a commercial beverage-can has been studied. The sample was immersed into a 0.005 M NaCl solution. The probe scans over a localized electrochemical event previously detected. The distance between tip reference and beverage-can surface was set at 80 μm. The scan area is 4.5 × 4 mm.
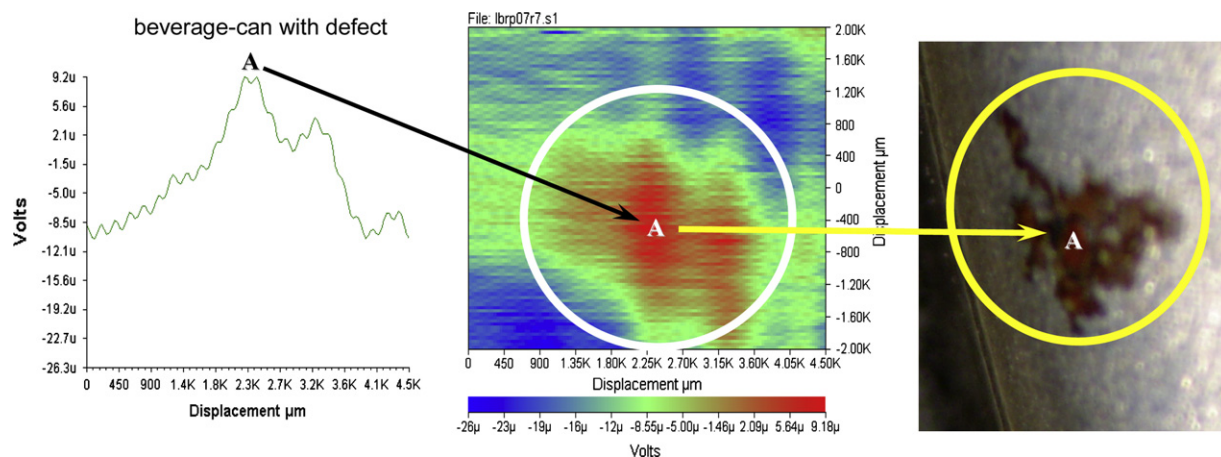
Fig. 16. Defect of the beverage-can base detected with the SVET technique.

The graph on the left of Fig. 16 is the SVET signal as measured in volts with the displacement in micrometers along the *x*-axis. The SVET map in the middle of Fig. 16 is a consecutive answer of several lines' scan that with time down the *y*-axis shows the measured signal in the form of defects of the coating. The dark area in the circle indicates an anodic behaviour, while zones outside could be interpreted as cathodic sites or intact coating. For comparison, an image of the corroded site is reported (Fig. 16, on the right). Observe that it is possible to see the defect just because this is a pigment-free coating. The growth of the local anode area on the paint film is statistically calculated and determined by the difference (ΔE) of the potential gradient values (E) between the local anode (defective area of painted film) and the local cathode part corresponding to a non-defective area. The E values for the anode part increase with the immersion time. The potential gradient value (E) could be converted into current density (i). The following are the calculations of the current density:

Curve response = 9.2 µV obtained from the graph (Fig. 16, on the left).

Applying the following equation it is easy to calculate the value of the current:

$$I = -\frac{1}{\rho}\frac{\Delta E}{2d} \qquad (17)$$

where ΔV is the output of the SVET, ρ is the conductivity of the solution and d is the vibration amplitude of the tip.

The solution conductivity is 12.47 µS cm^{-1}, hence:

$$R = \frac{1}{12.47 \ \mu S \ cm^{-1}} = 8.2 \times 10^{-3} \ \Omega \ cm^{-1}$$

Multiplying this value by the vibration amplitude of the probe tip: $8.2 \times 10^{-3} \ \Omega \ cm^{-1} \times 30 \ \mu m = 25 \ \mu\Omega$.

Using Ohm's Law: $E = IR$, $E = 9.2 \ \mu V$ and $R = 25 \ \mu\Omega$, $I = 23 \ nA$.

4. Summary

High resolution localized techniques such as SKP and SVET have been explained. The basic principles of these devices have been reported with some simple clarifying mathematical models. In addition, practical examples of the potential of these devices have been proposed in order show the wide application fields and the importance of the data achievable. It has been discussed that SVET provides very interesting information concerning the local values of the current and potential, and the experimental data are quite easy to correlate with the corrosion phenomena occurring at the metal interface. However, the limitation of this technique is that it is necessary to use an electrolyte. The presence of a conductive solution directly in contact with the sample affects the electrochemical activity of the surface of the metal. The achievable electrochemical data are influenced by the effect of the electrolyte on the natural evolution of the corrosion processes. On the contrary, SKP needs no contact between the sample and a conductive solution. Thus, the corrosion process can be monitored affecting just slightly the system. The limit of this device can be found in the difficulty of the interpretation of the experimental data.

References

[1] P. Marcus, Analytical Methods in Corrosion Science and Engineering, Marcel Dekker Inc., NY, United States, 2005.

[2] D.A. Jones, Principle and Prevention of Corrosion, Prentice Hall, New York, USA, 1996.

[3] P.L. Bonora, F. Deflorian, L. Fedrizzi, Electrochim. Acta 41 (1996) 1073.

[4] C. Zhong, X. Tang, Y.F. Cheng, Electrochim. Acta 53 (2008) 4740.

[5] B.B. Katemann, A. Schulte, E.J. Calvo, M. Koudelka-Hep, W. Schuhmann, Electrochem. Commun. 4 (2002) 134.

[6] J.H.W. de Wit, D.H. van Weijde, A.J. De Jong, F. Blekkenhorst, S.D. Meijers, Mater. Sci. Forum 289 (1998) 69.

[7] M. Rohwerder, F. Turcu, Electrochim. Acta 53 (2007) 290.

[8] X. Zhang, W.G. Sloof, A. Hovestad, E.P.M. van Westing, H. Terryn, J.H.W. de Wit, Surf. Coat Technol. 197 (2005) 168.

[9] L. Forget, J. Delhalle, Z. Mekhalif, Mater. Corros. 52 (2001) 181.

[10] K. Wapner, G. Grundmeier, Adv. Eng. Mater. 6 (2004) 163.

[11] T.H. Munster, A.E. Hughes, J. Electrochem. Soc. 153 (2006) B474.

[12] J. Elvins, A. JohnSpittle, D.A. Worsley, Corros. Sci. 47 (2005) 2740.

[13] S.G.R. Brown, N.C. Barnard, Corros. Sci. 48 (2006) 2291.

[14] D.A. Worsley, H.N. McMurray, A. Belghazi, Chem. Commun. (1997) 2369.

[15] J. He, V. Johnston Gelling, D.E. Tallman, G.P. Bierwagen, J. Electrochem. Soc. 147 (2000) 3661.

[16] A. Nazarov, D. Thierry, Electrochim. Acta 52 (2007) 7689.

[17] G. Klimow, N. Fink, G. Grumdmaier, Electrochim. Acta 53 (2007) 1290.

[18] D.J. Penney, J.H. Sullivan, D.A. Worsley, Corros. Sci. 49 (2007) 1321.

[19] J. He, V.J. Gelling, D.E. Tallman, G.P. Bierwagen, G.G. Wallace, J. Electrochem. Soc. 147 (2000) 3667.

[20] M.F. Montemor, A.M. Cabral, M.L. Zheludkevich, M.G.S. Ferreira, Surf. Coat. Technol. 200 (2006) 2875.

[21] G. Grundmeier, W. Schmidt, M. Stratmann, Electrochim. Acta 45 (2000) 2515.

[22] M. Stratmann, H. Streckel, Corros. Sci. 30 (1990) 681.

[23] M. Stratmann, H. Streckel, Corros. Sci. 30 (1990) 697.

[24] K.R. Tretheway, D.A. Sargeant, D.J. Marsh, A.A. Tamimi, Corros. Sci. 35 (1993) 127.

[25] K. Wapner, M. Stratmann, G. Grundmeier, Silicon Chem. 2 (2003) 235.

[26] J. Bonnet, L. Soonckindt, L. Lassabatère, Vacuum 34 (1984) 693.

[27] D. Zhu, W.J. Van Ooij, Corros. Sci. 45 (2003) 2177.

[28] F. Deflorian, S. Rossi, L. Fedrizzi, M. Fedel, Prog. Org. Coat. (2008). doi:10.1016/j.porgcoat.2008.03.005.

[29] F. Vacandio, Y. Massiani, P. Gravier, S. Rossi, P.L. Bonora, L. Fedrizzi, Electrochim. Acta 46 (2001) 3827.

[30] J.L. Luo, Y.C. Lu, M.B. Ives, Mater. Performance 31 (1992) 44.

[31] S.J. Bates, S.R. Gosden, D.A. Sargeant, Mater. Sci. Technol. 5 (1989) 356.

[32] I. Sekine, T. Suzuki, M. Yiasa, K. Handa, K. Takaoka, L. Silao, Prog. Org. Coat. 31 (1997) 185.

[33] U.R. Evans, J. Iron Steel Inst. 141 (1940) 219.

[34] H.S. Isaacs, B. Vyas, in: F. Mansfield, U. Bertocci (Eds.), Electrochemical Corrosion Testing, American Society for Testing and Materials, 1981, p. 3 ASTM STP727.

[35] D.A. Sargeant, J.G.C. Hainse, S.J. Bates, Mater. Sci. Technol. 5 (1989) 487.

[36] E. Bayet, F. Huet, M. Keddam, K. Ogle, H. Takenouti, Mater. Sci. Forum 289 (1998) 57.